Journal of Cellular Biochemistry 101:1023–1037 (2007)

L-type Voltage-Operated Ca^{+2} Channels Modulate Transient Ca^{+2} Influx Triggered by Activation of Sertoli Cell Surface L-Selectin

Tzu-Jen Kao and Clarke F. Millette*

Department of Cell and Developmental Biology and Anatomy,
University of South Carolina School of Medicine, Columbia, South Carolina 29209

Abstract Near the base of mammalian seminiferous epithelium, Sertoli cells are joined by tight junctions, which constitute the blood–testis barrier. Differentiating germ cells are completely enveloped by Sertoli cells and must traverse the tight junctions during spermatogenic cycle. Following the specific ligand activation of L-selectin, the up-regulated Rho family small G-proteins have been implicated as important modulators of tight junctional dynamics. Although the activation of L-selectin transmits subsequent intracellular signals in a Ca^{+2}-dependent fashion in various cell types, little is understood regarding the signaling pathways utilized by L-selectin in Sertoli cells. Therefore, we have examined the possible resultant calcium influx triggered by specific ligand-activation of cell surface L-selectin receptors or by cross-linking of L-selectin with anti-L-selectin. Spectrofluorimetric studies demonstrate increase of intracellular Ca^{+2} levels immediately after the treatment of the L-selectin ligands, fucoidan and sialyl Lewis-a, or after treatment with anti-L-selectin antibody. We then determined the mechanism of Ca^{+2} influx by investigating L- and T-type voltage-operated Ca^{+2} channels, which have been suggested to present in the membranes of Sertoli cells. Data demonstrate that Sertoli cells treated with L-type voltage-operated Ca^{+2} channel antagonists, nifedipine, diltiazem, or verapamil, lead to dose-dependent blockage of L-selectin-induced Ca^{+2} influx. Cells treated with mibedradil, a T-type voltage-operated Ca^{+2} channel antagonist, results in little or no blocking effect. Therefore, we conclude that activation of Sertoli cell L-selectin induces Ca^{+2} influx, which is at least partially regulated by L-type voltage-operated Ca^{+2} channels. J. Cell. Biochem. 101: 1023–1037, 2007.

Key words: Sertoli cells; Ca^{+2} influx; L-selectin; L-type Ca^{+2} channels

In mammalian seminiferous tubules, Sertoli cells constitute the somatic elements, forming a complex columnar epithelium that undergoes repetitive cyclic changes during the spermatogenic cycle. All stages of developing germ cells are completely enveloped and physically supported by Sertoli cells, which supply hormonal signals and nutrients essential for spermatogenesis. Near the base of seminiferous epithelium, tight junctions (TJs) occur between adjacent Sertoli cells to constitute the blood–testis barrier. These TJs compartmentalize the seminiferous epithelium into the basal compartment containing spermatids and differentiated spermatocytes [Mruk and Cheng, 2004]. TJs isolate and protect advanced germ cells, and must change regularly during the spermatogenic cycle to allow the translocation of the nonmotile germ cells into the adluminal region. Rho family small G-proteins (RhoA and Rac1) have been implicated directly in the regulation of Sertoli cell tight junctional dynamics by modulating actin cytoskeleton rearrangements [Freeman et al., 2002]. These data also demonstrated that the specific ligand activation of Sertoli cell surface L-selectin stimulates activation of the Rho small GTPases. However, the signaling pathways utilized by L-selectin in Sertoli cells have not yet been identified.

The selectins are a family of carbohydrate binding cell adhesion molecules comprised of

Grant sponsor: NIH; Grant number: HD-372800 (to CFM).

*Correspondence to: Dr. Clarke F. Millette, PhD, Department of Cell and Developmental Biology and Anatomy, University of South Carolina School of Medicine, 6439 Garners Ferry Road, Columbia, SC 29209. E-mail: clarke@med.sc.edu

Received 1 May 2006; Accepted 11 August 2006

DOI 10.1002/jcb.21135

three members, L-, E-, and P-selectin. These molecules effect adhesive interactions of leukocytes, endothelial cells, and platelets in a Ca^{+2}-dependent fashion to regulate diapedesis and lymphocyte homing [Ley, 2003; Simon and Green, 2005]. Each specific selectin is composed of a highly conserved extracellular N-terminal region containing a lectin-binding domain, an epidermal growth factor-like domain, and a variable number of short consensus repeats [Tedder et al., 1995]. The short intracellular regions at the C-terminus show low homology and may allow for specific functions [Pavalko et al., 1995; Kansas and Pavalko, 1996]. Of the three selectins, only L-selectin is constitutively expressed at the cell surface, and it is highly involved in early steps of lymphocyte homing and leukocyte extravasation during inflammation [Butcher, 1991; Springer, 1994]. Cross-linking of L-selectin with antibodies or ligation of L-selectin with ligands elicits various cellular events, including elevated intracellular Ca^{+2} level [Laudanna et al., 1994; Waddell et al., 1995] and small GTPase-mediated actin cytoskeletal rearrangements [Brenner et al., 1997; Roberts et al., 1999], in leukocytes.

Six voltage-operated Ca^{+2} channels (VOCCs), including T-, L-, N-, P-, Q-, and R-types, are distributed differentially depending upon cell type and localization. They are a major gateway of calcium translocation through the plasma membranes of excited cells and support various cellular functions including cell growth and regulation, cell motility, muscle contraction, and neurotransmitter and hormone release [Parys et al., 2000]. Among these Ca^{+2} channels, the most significant difference is between the T-type, known as low-voltage-activated channel and the others, known as high-voltage-activated channels. Additionally, each channel type exhibits distinct biophysical properties. At present, pharmacological differentiation is the best way to differentiate each type. Both L- and T-type Ca^{+2} channels have been suggested to present in the membrane of immature Sertoli cells and to be involved in several signal transduction pathways [Wassermann et al., 1992a; Lalevee et al., 1997; Fagnen et al., 1999; Taranta et al., 2000; Touyz et al., 2000; Volpato et al., 2004]. Although it is well known that L-selectin mediates its adhesive interaction in a Ca^{+2}-dependent fashion, the mechanism of intracellular Ca^{+2} shifts induced by L-selectin ligands has not yet been studied intensively [Nebe et al., 2002], and no such study has been reported involving Sertoli cells.

Previous data has demonstrated the presence of L-selectin within the testis, both in the Sertoli cells and in various stages of germ cells, and the activation of Rho family small GTPases when exposed to known L-selectin ligands [Broome et al., 1997; Freeman et al., 2002]. Hence, we postulate that activation of L-selectin results in Ca^{+2} influx in Sertoli cells, and that this change in Ca^{+2}, in turn, could increase subsequent small GTPase activity. In this report, we investigate whether L-selectin activation using two different L-selectin ligands, fucoidan and sialyl Lewis-a, as well as anti-selectins results in the triggering of Ca^{+2} influx. Additional control experiments were performed to demonstrate the specific co-relation between the activation of L-selectin and the generation of an increased $[Ca^{+2}]_i$ transient. Finally, the mechanism of Ca^{+2} influx induced by L-selectin ligands were also investigated using both L- and T-type VOCC antagonists.

MATERIALS AND METHODS

Materials

Hank's balanced salt solution (HBSS), antibiotic–antimycotic, penicillin L-glutamine, and Trypsin-EDTA were from Gibco (Grand Island, NY). Dulbecco's modified Eagle's medium (DMEM)/F-12 Ham without phenol red, dimethyl sulfoxide (DMSO), fucoidan, nifedipin, (±)-verapamil hydrochloride (verapamil), diltiazem hydrochloride (diltiazem), and mibefradil dihydrochloride (mibefradil), were purchased from Sigma (St. Louis, MO). Pluronic F-127 stock solution (20% (w/v)) in DMSO, Fura Red acetoxymethyl (AM) esters, and fluo-3 AM esters were obtained from Molecular Probes (Eugene, OR). L-selectin (N-18), L-selectin (H-149), and P-selectin (CTB201) antibodies were provided by Santa Cruz (Santa Cruz, CA). Sialyl Lewis-a and sialyl Lewis-x were purchased from Toronto Research Chemicals (North York, ON, Canada). Fetal bovine serum (FBS) was from Atlanta Biologicals (Norcross, GA). Thapsigargin was provided by Calbiochem (San Diego, CA).

Animals

All animals were housed in the University of South Carolina School of Medicine Animal Facility. Procedures for animal sacrifice were

approved through the Institutional Animal Care and Use Committee at the University of South Carolina. Animals were sacrificed by CO_2 inhalation followed by cervical dislocation.

Cell Culture and Cell Isolation

Sertoli cells of 16–20-day old rats were isolated by sequential enzyme digests according to modifications of Okanlawon and Dym [1996]. Briefly, immature Sertoli cells (SCI) were isolated from 16–20-day old CD Albino rats (Harlan Sprague–Dawley) through sequential enzyme digests. All enzyme digests were carried out at 30°C in a shaking water bath set to 135 reciprocal oscillations per minute. Tubules were washed at least three times between each digest in HBSS. The cells were then pelleted, washed, and plated to 60×15-mm cell culture dishes with 5% FBS medium. At 24 h after plating, media was aspirated and replaced with 3 ml free media.

ASC-17D cells, an adult rat Sertoli cell line, were originally immortalized with a temperature-sensitive mutant of the SV40 virus, tsA225, which is active at 33°C and inactive at 40°C [Roberts et al., 1995]. ASC-17D cells and primary Sertoli cells were fed with DMEM/F-12 without phenol red supplemented with 5% fetal bovine serum, 2% antibiotic–antimycotic, and 2% penicillin L-glutamine. All cells were maintained in a humidified incubator in an atmosphere of 95% air and 5% CO_2, at 33°C.

Calcium Dye Loading

Primary Sertoli cell cultures or ASC-17D cells were first starved with serum-free DMEM medium. After 16–24 h, cells were trypsinized and counted with a hemocytometer. Cultures were then incubated with loading buffer containing 130 mM NaCl, 5 mM KCl, 1 mM Na_2HPO_4, 1 mM $CaCl_2$, 1 mM $MgCl_2$, and 25 mM Hepes (pH 7.4). Cells were loaded with two high-affinity Ca^{+2} BAPTA dyes, 2 μM fluo-3 and/or 6 μM Fura Red acetoxymethyl (AM) esters according to modifications of Lyng et al. [2000]. When bound to Ca^{+2}, the fluorescence intensity of fluo-3 at a wavelength of 525 nm increases, but that of Fura Red at 660 nm decreases. Fluo-3 and Fura Red AM esters were dissolved in DMSO and mixed with 20% (w/v) Pluronic F-127 stock solution in DMSO at a ratio of 1:1 immediately before use. Dilutions were made in loading buffer so the final concentration of DMSO was less than 0.1%. Cells were incubated with dye in the buffer at 33°C for an hour before washing away excess dye. Samples were then incubated for an additional 30 min to allow intracellular dye deesterification. Cells were diluted to 3×10^6 per ml with loading buffer. In all experiments, the water used for buffers was of HPLC grade, having passed through multiple deionizers and organic removal filters in a Barnstead E-Pure processing unit. Resultant conductance values consistently measured 17.4 megaohms-cm.

Dose–Response Calcium Measurements by Spectrofluorimetry

Three types of dose–response calcium measurements were conducted: *ligand specificity*, *anti-selectin*, and *Ca^{+2} channel blocker* experiments. Each set of experiments using different cell types, different external [Ca^{+2}], different stimulating ligands or channel blockers, and different dosages of ligands/blockers was repeated at least three times to five times. Each experimental replicate was completely independent from every other; meaning, for example, that fresh cell isolates were used for each individual replicate study. Statistical analysis was completed (see below). Statistical variation between individual experiments was not significant (data not shown). Therefore, for clarity, a single representative experiment for each treatment has been shown. For *ligand specificity* experiments, 1 ml of dye-loaded cell suspension was placed into a plastic cuvette followed by adding 1 ml of loading buffer containing additional 0–100 nM of free Ca^{+2}. The cuvette was then inserted into a FluoroMax-3 spectrofluorimeter (Jobin Yvon, Edison, NJ), and an additional 1 ml of selected reagent, [thapsigargin, fucoidan, sialyl Lewis-a or -x], was added into the cuvette immediately before Ca^{+2} determinations [excitation wavelength set at 488 nm] to make 3 ml of final solution with 10^6 cells per trial. Emission wavelength scans were then taken from 500 nm to 800 nm at 1-nm intervals, with a total fluorescence integration time set at 0.025 s per wavelength. Total measurement time, therefore, was about 7.5 s. Since no usable emission data were acquired between 700 and 800 nm, only results from 500 to 700 nm have been shown, representing a total measurement time of about 5 s. The fluorescence intensity of loading buffer only was measured prior to each set of experiments to serve as blank. Each control blank determination was subtracted

from the experimental result automatically to correct for background fluorescence. Resultant data were displayed as plots of fluorescence intensity versus wavelength. A significant absorption peak [fluo-3] peak was detected at 525 nm, as was a much smaller Fura Red peak [660 nm]. Ratio plots shown were created by comparing experiments with reagents added to those without reagents under the same conditions to identify changes in intracellular [Ca^{+2}].

For *anti-selectin* experiments, the basic setup was the same, but SCI or ASC-17D cells were loaded with 2 μM fluo-3 only and diluted with loading buffer. One of three anti-selectins, including L-selectin antibodies specific for peptide sequences in either the N- or C-terminus, and a P-selectin antibody, was added into the cuvette in 1:100 dilutions immediately before each Ca^{+2} determination. For *Ca^{+2} channel blocker* experiments, cells loaded with 2 μM fluo-3 were incubated with various concentrations of nifedipine, verapamil, diltiazem, or mibefradil at 33°C for 10 to 20 min before completion of the experimental protocol described for the *ligand specificity* studies. Nifedipine was dissolved in acetone, verapamil was dissolved in methanol, and diltiazem and mibefradil were dissolved in loading buffer prior to experiments. For both *anti-selectin* and *Ca^{+2} channel blocker* experiments, resultant data were displayed as plots of fluorescence intensity versus wavelength.

Real-Time Calcium Measurements by Spectrofluorimetry

For *real-time measurements*, experiments were set up the same way and while the excitation wavelength was still set at 488 nm, the emission wavelengths were also set at 525 nm for fluo-3 and 660 nm for Fura Red. Selected reagents, including BSA, fucoidan, sialyl Lewis-a or sialyl Lewis-x, were added after 2-min baseline measurements. Resultant Ca^{+2} changes were monitored for 15 min. Measurements were completed using automatic switching between 525 nm and 660 nm at 2 s intervals. Thus, two plots of fluorescence intensity versus time for each fixed wavelength were obtained per experiment, and the ratio was then calculated and plotted with Excel. Again, each experiment was repeated from three–five times, in completely independent conditions, with little or no statistically significant differences noted between replicates. Therefore, as before, single representative experiments were chosen for presentation.

Statistical Analysis

Data from the experimental replicate sets were evaluated using GraphPad PRISM 4 (GraphPad Software, Inc., San Diego, CA). Means of the combined ratio from the *ligand-specificity* experiments and of the integrated areas under each fluorescence peak from the *anti-selectin* and *Ca^{+2}-channel blocker* experiments were compared respectively using Student's unpaired *t*-tests with the threshold for statistical significance set at $P < 0.05$. In a few instances, indicated in the text, significance levels were detected only at $P < 0.1$ for particular experimental sets.

RESULTS

Ca^{+2} Influx Stimulated by Activation of L-Selectin

Spectrofluorimetric fluorescence measurements were performed to determine the effect on Ca^{+2} influx by fucoidan and sialyl Lewis-a, two L-selectin ligands. Figure 1 (panel A) compares the ratio of untreated control [ctrl]/100 nM Ca^{+2} to the ratio of ctrl/100 nM Ca^{+2} loaded with 4 μM thapsigargin using primary Sertoli cell isolates (SCI). Substantial Ca^{+2} influx is indicated by the ratio decrease at 525 nm and its increase at 660 nm, representing increased fluo-3 and decreased Fura Red absorbance. Thapsigargin, an ionophore that increases intracellular Ca^{+2} levels dramatically by both inhibiting endoplasmic reticular Ca^{+2}-ATPase and activating cell-surface voltage-dependent and voltage-independent Ca^{+2} channels to induce Ca^{+2} influx, serves as a maximum positive control [Lyles et al., 1998; Thomas et al., 1999; Balema et al., 2006]. Figure 1 (panel B) compares the ratio of ctrl/100 nM Ca^{+2} to the ratio of ctrl/100 nM Ca^{+2} loaded with 200 μg/ml fucoidan. Here, a resultant Ca^{+2} influx is indicated primarily by the ratio decrease at 525 nm; differences in the fluorescence ratios in the Fura Red range (660 nm) are less obvious.

Similar experiments were repeated using ASC-17D cells with 10 nM free Ca^{+2} included (Fig. 1C,D), and positive indications for resultant Ca^{+2} were noted, in excellent agreement with the findings using SCI. Results of cellular activation using thapsigargin versus fucoidin were virtually indistinguishable. Figure 1

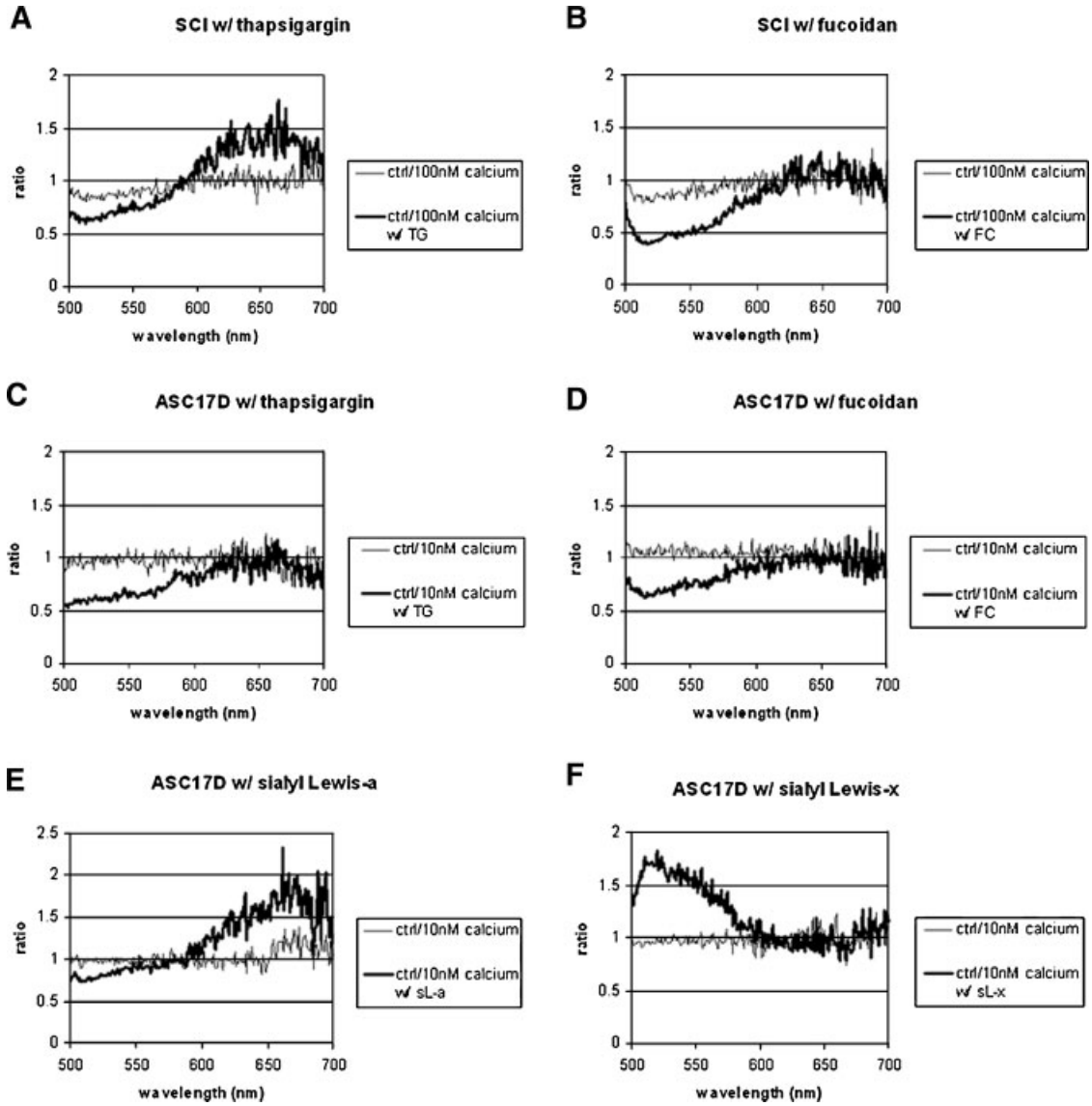

Fig. 1. Ligand-specificity analysis of Ca^{+2} spectrofluorimetric fluorescence measurements using ASC-17D cells and immature Sertoli cells. Each panel compares two ratio plots. One plot is the ratio of (a) a control containing loading buffer with minimal free Ca^{+2} and no reagent to (b) a control having 10 nM free Ca^{+2}. The second plot (bolded) displays the ratio of (a) a control with loading buffer only to (b) a sample containing 4 μM thapsigargin (panels **A** and **C**), 200 μg/ml fucoidan (panels **B** and **D**), 30 μM sialyl Lewis-a (panel **E**), or 30 μM sialyl Lewis-x (panel **F**). The free calcium levels displayed (100 nM for SCI cells; 10 nM for ASC-17D cells) represent optimum levels as determined by dose–response assays. Fluorescence intensity, which is proportional to intracellular levels of Ca^{+2}, was measured with a spectrofluorimeter after loading cells with 2 μM fluo-3 and 6 μM Fura Red as indicated in Materials and Methods. Statistical analysis indicated that significant differences ($P < 0.05$) were always detected at 525 nm between the two ratios. At 660 nm, significant differences were always seen, but at $P < 0.1$.

(panel E) compares the ratio of ctrl/100 nM Ca^{+2} to the ratio of ctrl/100 nM Ca^{+2} loaded with 30 μM sialyl Lewis-a, a ligand specific for L-selectin. Again, results demonstrate a clear influx of Ca^{+2} with data completely comparable to those seen using SCI cells activated by thapsigargin (compare panels A,E). Finally, using ASC-17D cells, (panel F) compares the ratio of ctril/100 nM Ca^{+2} to the ratio of ctrl/100 nM Ca^{+2} loaded with 30 μM sialyl Lewis-x, instead of sialyl-Lewis a. Sialyl Lewis-x is a specific ligand for E- and P-selectin. It does not activate L-selectin and, therefore, serves as a negative control. Note that no Ca^{+2} influx is detected here, as indicated by an elevated, rather than lessened, fluorescence ratio for

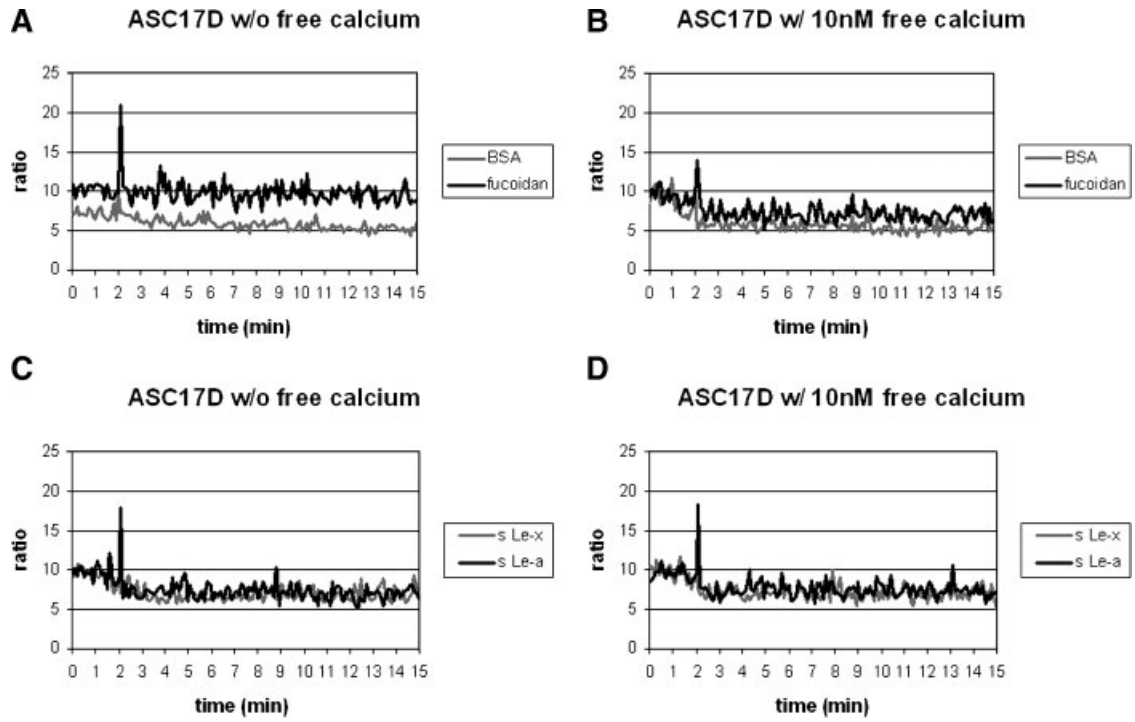

Fig. 2. Real-time analysis of Ca^{+2} spectrofluorimetric fluorescence measurements using ASC-17D cells. Panels **A** and **B** compare the ratio of [fluo-3/Fura Red] in the presence of 200 μg/ml BSA with the ratio obtained by adding the same concentration of fucoidan, without or with 10 nM free Ca^{+2} included. Results from fucoidan studies are indicated by the bolded plot. Panels **C** and **D** compare the ratio of [fluo-3/Fura Red] in the presence of 30 μM sialyl Lewis-x with the ratio obtained using the same amount of sialy Lewis-a, without or with 10 nM free Ca^{+2} included. Results obtained using sialyl-Lewis-a are indicated by the bolded plots. Reagents were injected into the cuvette after measuring baseline levels for 2 min, and samples were then monitored for 15 min. Increased $[Ca^{+2}]_i$ transients are demonstrated by the sharp peak seen at times between 2 and 3 min of observation. These peaks are seen only with ligands known to bind L-selectin.

fluo-3; and no notable increase in fluorescence ratio for Fura Red.

While no specificity controls for fucoidin stimulation have been shown here, previous data from this laboratory using both alternate glycosylated proteins in place of fucoidin, or deglycosylated fucoidin itself, have demonstrated that L-selectin on either ASC-17D cells or Sertoli cells cannot be activated. Moreover, real-time measurements studies (Figs. 2 and 3, below) do show data using bovine serum albumin as a negative control for fucoidin.

Statistical analysis indicated that significant differences ($P < 0.05$) were always detected at 525 nm between the two ratios. At 660 nm, significant differences were always seen, but at $P < 0.1$. An unexpected effect of sialyl Lewis-x at 525 nm (Fig. 1F) indicates a decrease of intracellular Ca^{+2} levels. While reproducible from experimental replicate to replicate, the mechanistic basis for this finding remains unclear and will require further study.

Real-Time Measurement of Ca^{+2} Influx

Real-time spectrofluorimetric fluorescence measurements were then performed to examine the Ca^{+2} influx induced by fucoidan and sialyl Lewis-a. Reagents were injected into the cuvette after 2-min baseline measurements, and samples were monitored for an additional 15 min. Figure 2 (panel A) compares the ratios of [fluo-3/Fura Red] in the presence of 200 μg/ml BSA or fucoidan without 10 nM free Ca^{+2} included using ASC-17D cells. BSA is used a control for non-specific protein interactions with the cell surface. It should not induce ion influx. Data demonstrate that the ratio for fucoidan increases twofold for a duration of no more than 6 s immediately after the addition of fucoidan. The ratio then returns to the original level. The ratio for BSA, however, shows little or no increase at any time following reagent addition, suggesting that induced Ca^{+2} influx is indeed specific for activation by L-selectin

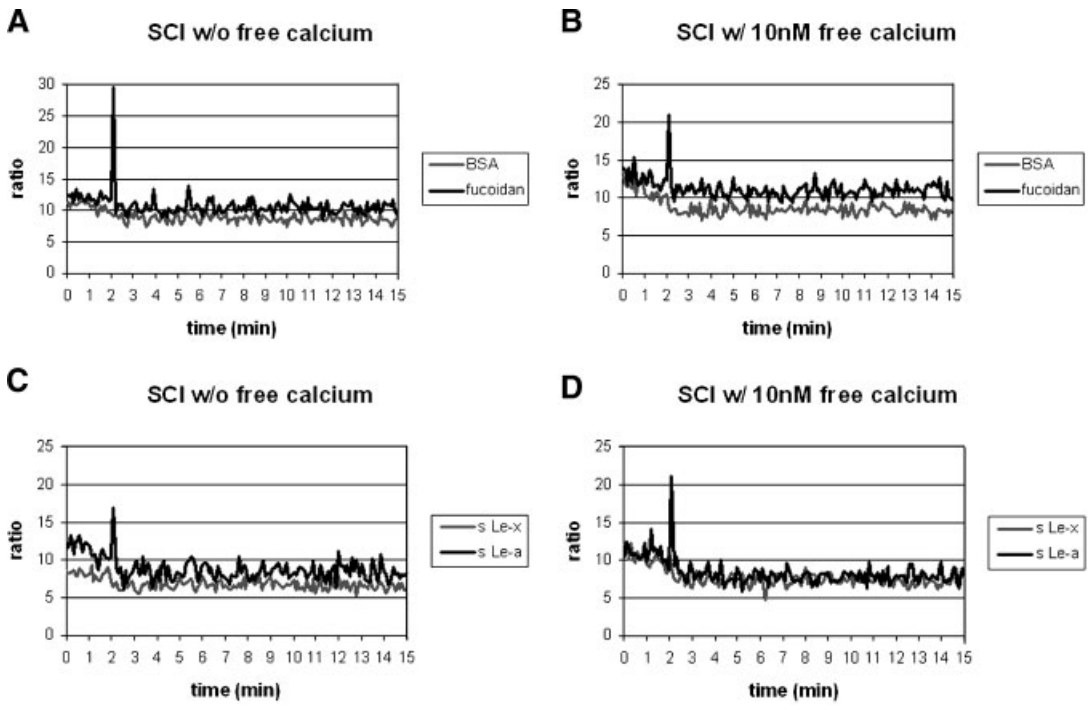

Fig. 3. Real-time analysis of Ca^{+2} spectrofluorimetric fluorescence measurements using immature Sertoli cells. **Panels A** and **B** compare the ratio of [fluo-3/Fura Red] in the presence of 200 μg/ml BSA with the ratio obtained by adding the same concentration of fucoidan, without or with 10 nM free Ca^{+2} included. Results from fucoidan studies are indicated by the bolded plot. **Panels C** and **D** compare the ratio of [fluo-3/Fura Red] in the presence of 30 μM sialyl Lewis-x with the ratio obtained using the same amount of sialyl Lewis-a, without or with 10 nM free Ca^{+2} included. Results obtained using sialyl Lewis-a are indicated by the bolded plots. Increased $[Ca^{+2}]_i$ transients are demonstrated by the sharp peak seen at times between 2 and 3 min of observation. These peaks are seen only with ligands known to bind L-selectin.

ligands. Experiments were then repeated with 10 nM free calcium included (Fig. 2B). The ratio for fucoidan shows a lesser but still significant increase compared with the result of Figure 2A. Again, BSA has no effect. Figure 2 panels C and D show rapidly increased ratios for no more than 6 s in the presence of 30 μM sialyl Lewis-a, without or with 10 nM free Ca^{+2} included. In contrast, addition of sialyl Lewis-x has no effect (panel D).

Additional real-time measurements with SCI were performed to determine the effect of Ca^{+2} influx (Fig. 3). The ratios for both fucoidan and sialyl Lewis-a show strong positive but transient results, and for both BSA and sialyl Lewis-x, there is little or no effect. Thus, findings for ASC-17D and SCI cells were comparable.

Effect of Ca^{+2} Influx by Anti-Selectins

Cell surface L-selectin may also be activated by antibody cross-linking and previous data using leucocytes indicates that such cross-linking also induces Ca^{+2} influx. Therefore, we tested the effects of adding anti-selectins on Ca^{+2} influx using both ASC-17D and SCI cells. Data represent dose–response experiments with cells exposed to one of three antibodies in 1:100 dilutions: L-selectin antibodies specific for peptide sequences in either the N- or C-terminus, and a P-selectin antibody that does not recognize L-selectin. Cell solutions containing minimal (Fig. 4A,D), 10 nM (Fig. 4B,E), and 100 nM (Fig. 4C,F) free Ca^{+2} were compared to determine the activating effects of these antibodies on Ca+2 influx. Because cells in these experiments were loaded with 2 μM fluo-3 only, results are shown as plots of fluorescence intensity versus wavelength range from 500 nm to 600 nm.

The N-terminus of L-selectin locates to the extracellular receptor domain. The C-terminus is positioned in the intracellular domain, however, and would be unavailable to external antibodies in our studies using intact, living cells. Therefore, a resultant alteration of intracellular $[Ca^{+2}]$ should be noted only after

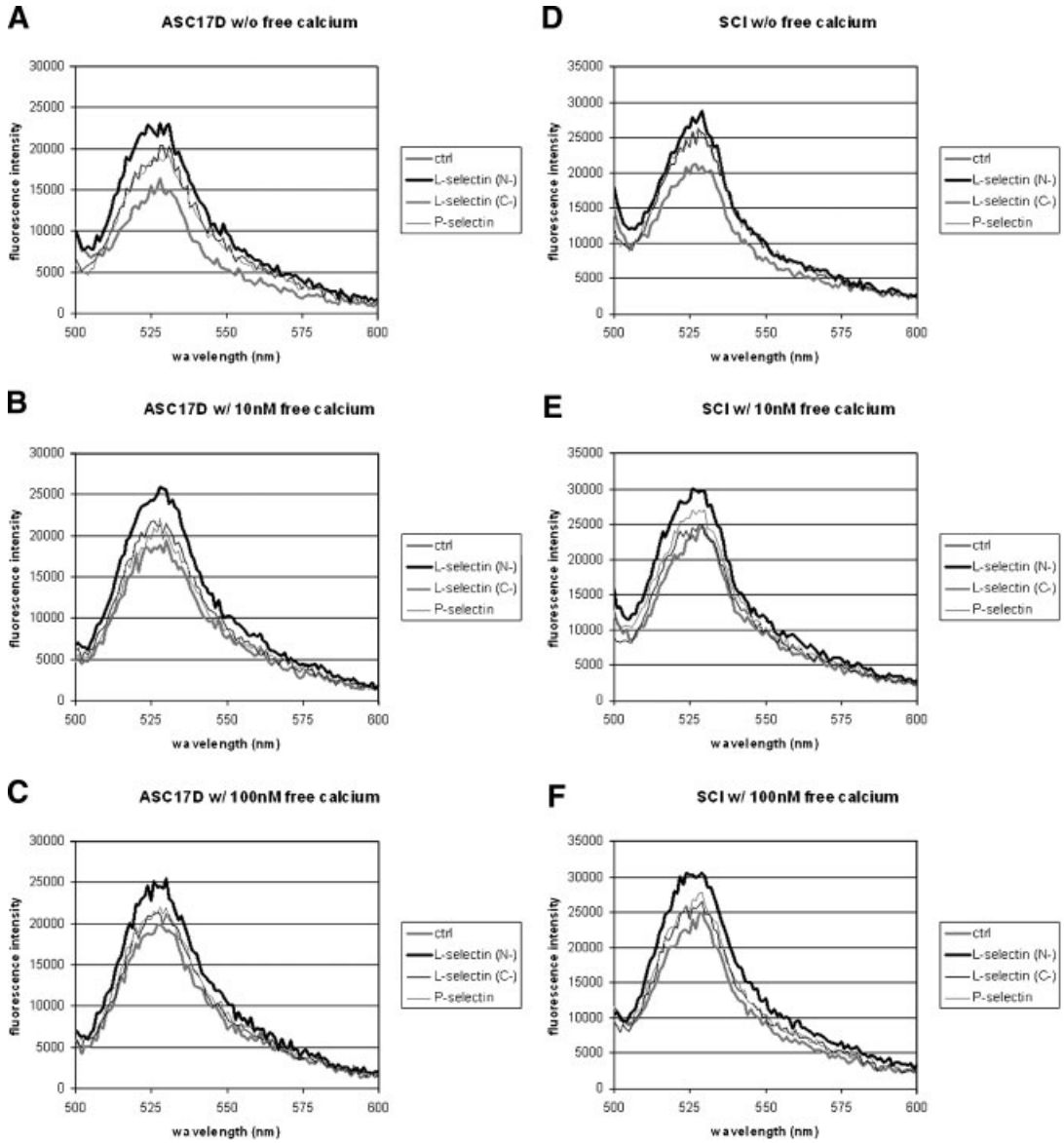

Fig. 4. Analysis of Ca^{+2} spectrofluorimetric fluorescence measurements using ASC-17D cells and immature Sertoli cells treated with anti-selectins. Cell solutions containing minimal (panels **A** and **D**), 10 nM (**panels B** and **E**), and 100 nM (**panels C** and **F**) added free Ca^{+2} were exposed to 1:100 dilutions of L-selectin antibody specific for peptide sequences in either the N- or C-terminus, or P-selectin antibody to compare their activating effects on Ca^{+2} influx. A control exposed to loading buffer is also included in each panel. Fluorescence intensity was measured after loading cells with 2 μM fluo-3 only and results are shown as plots of fluorescence intensity versus wavelength. In all panels, the bolded plot represents the increased Ca^{+2} influx obtained in the presence of the only agent expected to activate cell surface L-selectin (anti-L-selectin N-terminus). Statistical analysis revealed that at free [Ca^{+2}] of 10 nM or higher, significant differences ($P < 0.05$) were always detected with experimental sets using anti-L-selectin N-terminal domain. Under these conditions (>10 nM external Ca^{+2}), statistically significant differences between controls and either anti-L-selectin C-terminal domain or anti-P-selectin were never detected.

addition of the anti-L-selectin specific for the N-terminus. Indeed, as shown in all panels of Figure 4, the fluorescence intensities for the L-selectin antibody against the N-terminus are the highest among all three antibodies, with the intensities 10–15% more than the other two antibodies. The fluorescence intensities for L-selectin antibody against C-terminus and those for P-selectin antibodies have mixed results, and controls treated with loading buffer always have the lowest fluorescence intensities. Statistical analysis revealed that at free [Ca^{+2}] of 10 nM or higher, significant differences ($P < 0.05$) were always detected with experi-

mental sets using anti-L-selectin N-terminal domain. Under these conditions (>10 nM external Ca^{+2}), statistically significant differences between controls and either anti-L-selectin C-terminal domain or anti-P-selectin were never detected. These findings demonstrate that only anti-L-selectin reagent specific for extracellular structural domains of this cell adhesion molecule can consistently induce influx of Ca^{+2}.

Effect of Ca^{+2} Influx by Ca^{+2} Channel Antagonists

ASC-17D cells were loaded with L- and T-type Ca^{+2} channel blockers to investigate identity of the membrane ion channels mediating Ca^{+2} influx induced by L-selectin ligands. Cells were incubated with 1, 3, or 5 μM nifedipine, a L-type Ca^{+2} channel blocker, after 2 μM fluo-3 loading. Figure 5 (panels A,B) compare the fluorescence intensities of cells loaded with 200 μg/ml fucoidan in the presence of nifedipine without or with 100 nM free Ca^{+2} included. Controls without nifedipine show progressive increase of intensity in the presence of fucoidan and/or 100 nM free Ca^{+2}. Upon the treatment of nifedidpine, fluorescence intensity decreases by 20–30%. Treatment with 3 μM nifedipine shows the most significant blockage of Ca^{+2} influx compared with those of 1 μM and 5 μM nifedipine. In companion studies, cells were then treated with 30 μM sialyl Lewis-a instead of fucoidin. Here, controls show normal progressive increase of fluorescence intensity (Fig. 5C,D). Addition of 3 μM nifedipine shows the strongest inhibition of ion influx, while 5 μM nifedipine has a more significant effect than does 1 μM nifedipine. Statistical analyses of these data reveal that at 3 μM nifedipine, significant differences were always detected at $P < 0.05$, independent of external Ca^{+2}. However, at 5 μM nifedipine, statistically significant levels were slightly dependent upon external Ca^{+2}. With no additional added ion, statistical differences were detected at $P < 0.1$; using 100 nM Ca^{+2}, significant differences were detected at $P < 0.05$.

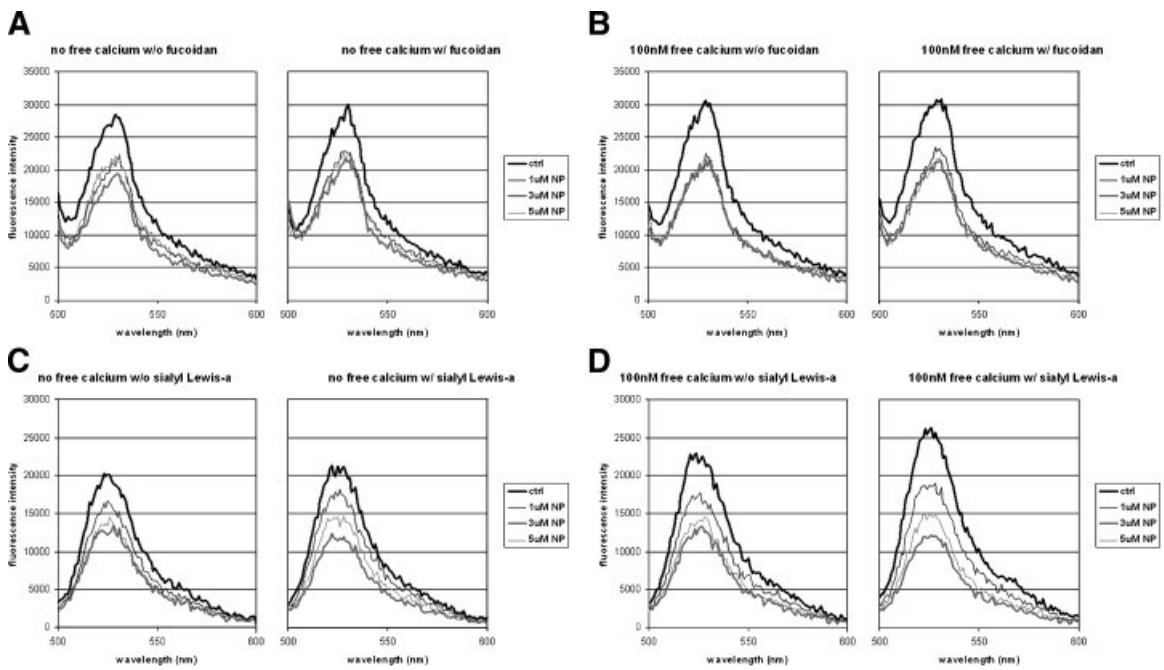

Fig. 5. Analysis of Ca^{+2} spectrofluorimetric fluorescence measurements using ASC-17D cells treated with nifedipine (NP), an L-type Ca^{+2} channel blocker. Cells were incubated with 1, 3, or 5 μM nifedipine for 15 min prior to fluorescence measurements. Each panel compares two groups of plots with or without addition of 200 μg/ml fucoidan (**panels A** and **B**) or 30 μM sialyl Lewis-a (panels **C** and **D**) in the presence of minimal or 100 nM free Ca^{+2}. Cells were loaded with 2 μM fluo-3 and results are shown as plots of fluorescence intensity versus wavelength. In all panels, the bolded plot represents the control without the treatment of nifedipine. Note the significant and dose-dependent decreases in $[Ca^{+2}]_i$ resultant from inclusion of nifedipine. Statistical analyses of these data reveal that at 3 μM nifedipine, significant differences were always detected at $P < 0.05$, independent of external Ca^{+2}. However, at 5 μM nifedipine, statistically significant levels were slightly dependent upon external Ca^{+2}. With no additional added ion, statistical differences were detected at $P < 0.1$; using 100 nM Ca^{+2} significant differences were detected at $P < 0.05$.

All in all, the data demonstrate the involvement of L-type Ca^{+2} channels in the downstream intracellular effects of L-selectin activation.

Two more L-type Ca^{+2} channel blockers, diltiazem and verapamil, were utilized to confirm the specific involvement of L-type Ca^{+2} channels. Cell solutions were incubated with 5, 10, and 20 (M diltiazem prior to measurements. Addition of 10 μM diltiazem results in the strongest inhibition of Ca^{+2} influx, lowering the fluorescence intensity 30–40% (Fig. 6). Expected dose–response data were obtained using both fucoidin and sialyl Lewis-a as L-selectin ligands. Statistical analysis of the fucoidin data here demonstrated that using 5 μM or higher levels of diltiazem always resulted in significant differences ($P < 0.05$) where expected, independent of external ion levels. Using sialyl Lewis-a, significant differences were found at $P < 0.1$ using 5 μM diltiazem and at $P < 0.05$ for inhibitor levels of 10 μM or greater. Cells were also treated with 1, 5, and 10 μM verapamil. These experiments reveal that the most significant inhibition is caused by 10 μM verapamil (Fig. 7). The results for both diltiazem and verapamil are very similar to those obtained using nifedipine. Statistical analysis here demonstrated that to achieve significant difference levels of $P < 0.05$ at least 5 μM verapamil were required. Added blocker at only 1 μM yielded significance values at $P < 0.1$. These data, therefore, confirm the involvement of L-type Ca^{+2} channels.

Finally, studies were designed to examine the potential involvement of T-type Ca^{+2} channels (Fig. 8). Mibefradil, a Ca^{+2} channel blocker with higher affinity for T-type (Kd = 0.1–4.7 μM) than L-type (Kd = 1.4-28 μM) Ca^{+2} channels, is often used to discriminate T-type from L-type Ca^{+2} channels [Ertel et al., 1997; Martin et al., 2000]. ASC-17D cells were loaded with 0.5, 1, and 5 μM mibefradil prior to fluorescence measurements. The results for 0.5 and 1 μM mibefradil show little or no difference compared with controls without mibefradil, demonstrating little or no involvement of T-type Ca^{+2}

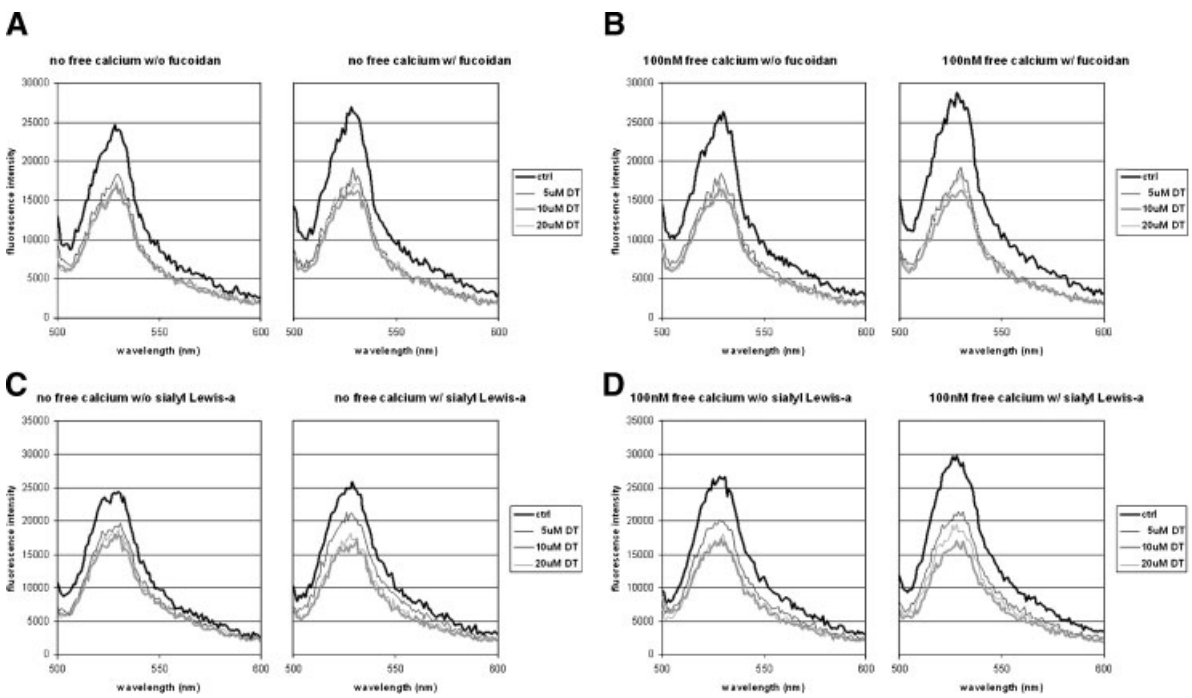

Fig. 6. Analysis of Ca^{+2} spectrofluorimetric fluorescence measurements using ASC-17D cells treated with diltiazem (DT), an L-type Ca^{+2} channel blocker. Cells were incubated with 5, 10, or 20 μM diltiazem for 15 min prior to fluorescence measurements. Each panel compares two groups of plots with or without addition of 200 μg/ml fucoidan (**panels A** and **B**) or 30 μM sialyl Lewis-a (**panels C** and **D**) in the presence of minimal or 100 nM free Ca^{+2}. Cells were loaded with 2 μM fluo-3 and results are shown as plots of fluorescence intensity versus wavelength. In all panels, the bolded plot represents the control without the treatment of diltiazem. Note the significant and dose-dependent decreases in $[Ca^{+2}]_i$ resultant from inclusion of diltiazem. Statistical analysis of the fucoidin data here demonstrated that using 5 μM or higher levels of diltiazem always resulted in significant differences ($P < 0.05$) where expected, independent of external ion levels. Using sialyl-Lewis-a, significant differences were found at $P < 0.1$ using 5 μM diltiazem and at $P < 0.05$ for inhibitor levels of 10 μM or greater.

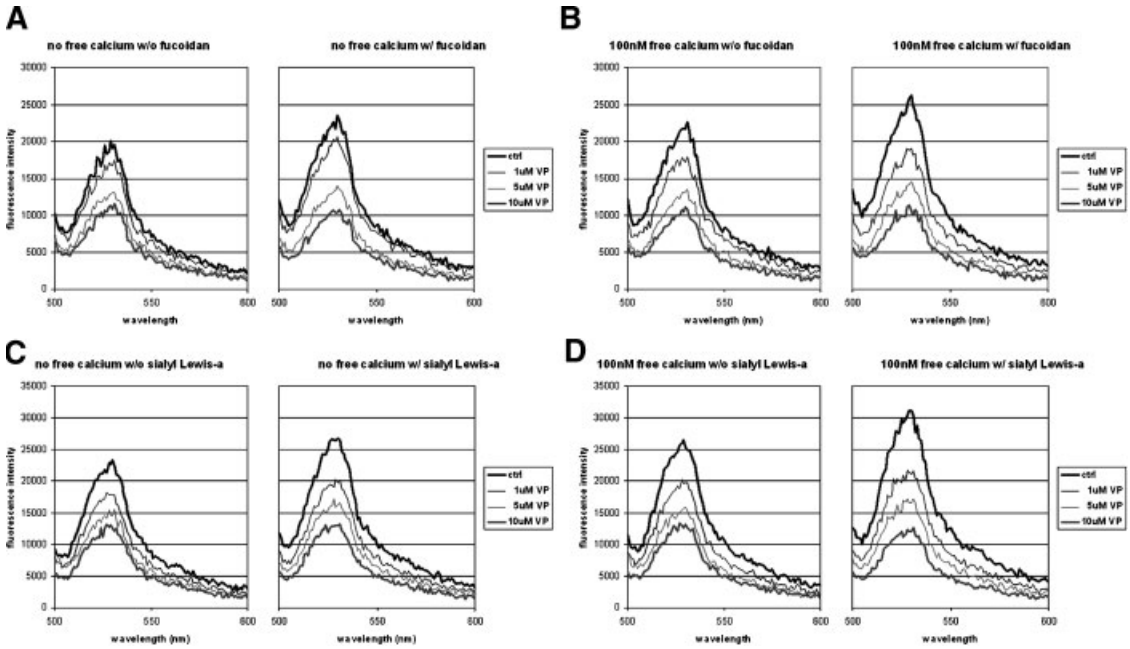

Fig. 7. Analysis of Ca^{+2} spectrofluorimetric fluorescence measurements using ASC-17D cells treated with verapamil (VP), an L-type Ca^{+2} channel blocker. Cells were incubated with 1, 5, or 10 μM verapamil for 15 min prior to fluorescence measurements. Each panel compares two groups of plots with or without addition of 200 μg/ml fucoidan (**panels A** and **B**) or 30 μM sialyl Lewis-a (**panels C** and **D**) in the presence of minimal or 100 nM free Ca^{+2}. Cells were loaded with 2 μM fluo-3 and results are shown as plots of fluorescence intensity versus wavelength. In all panels, the bolded plot represents the control without the treatment of verapamil. Note the significant and dose-dependent decreases in $[Ca^{+2}]_i$ resultant from inclusion of verapamil. Statistical analysis here demonstrated that to achieve significant difference levels of $P < 0.05$ at least 5 μm verapamil were required. Added blocker at only 1 μM yielded significance values at $P < 0.1$.

channels. The result for 5 μM mibefradil, however, shows an apparent slightly decreased fluorescence intensity when compared with the other three groups. This seeming partial inhibition could result from the known non-specificity of mibefradil at higher concentrations, where both T-type and L-type channels may be blocked. However, analysis of these data demonstrated that the apparent slight inhibition at 5 μM mibefradil was never statistically significant.

DISCUSSION

The activation of cell surface L-selectin receptor via interaction with its ligands has been shown to trigger a transient increase of intracellular Ca^{+2} levels in leukocytes to transmit various intracellular signals [Laudanna et al., 1994; Norgard-Sumnicht et al., 1993; O'Connell et al., 1996]. However, no existing data describe cytosolic Ca^{+2} increases triggered by Sertoli cell surface L-selectin activation. Here, experiments determined that ligation of Sertoli cell surface L-selectin is indeed able to induce an increase in $[Ca^{+2}]_i$. Additionally, real-time experiments were performed to determine the duration of this $[Ca^{+2}]_i$ increase. By comparing the ratios before and after the exposure of either fucoidan or sialyl Lewis-a to cells loaded with Ca^{+2} indicator dyes, an increase of intracellular Ca^{+2} level was detected in the presence of each of these specific activating ligands. Control experiments with thapsigargin showing maximal effects and sialyl Lewis-x showing null effects confirmed the selectiveness of ligation. Furthermore, by comparing the fluorescence ratio of two loaded Ca^{+2} dyes, results of real-time measurements demonstrated that the duration of $[Ca^{+2}]_i$ increases last for no more than 10 s after addition of L-selectin ligand. Control experiments with BSA and with sialyl Lewis-x showing little or no increase of intracellular Ca^{+2} levels further confirmed the specificity of the observed transient $[Ca^{+2}]_i$ changes. The transient increase of cytosolic Ca^{+2} level suggests that it is likely to be involved in downstream signal transduction pathways triggered by ligation of Sertoli cell surface L-selectin receptor. Previous studies have shown, for example, that the activation of Rho small

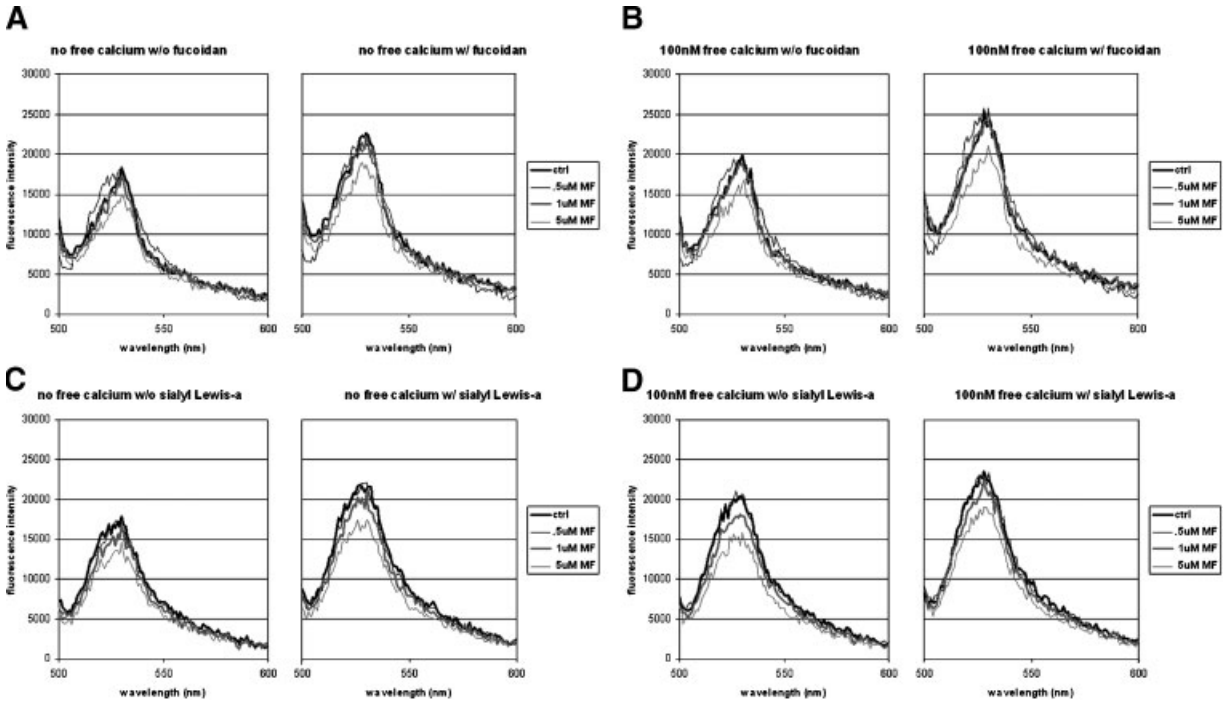

Fig. 8. Analysis of Ca^{+2} spectrofluorimetric fluorescence measurements using ASC-17D cells treated with mibefradil (MF), a T-type Ca^{+2} channel blocker. Cells were incubated with 0.5, 1, or 5 μM mibefradil for 10 min prior to fluorescence measurements. Each panel compares two groups of plots with or without addition of 200 μg/ml fucoidan (**panels A** and **B**) or 30 μM sialyl Lewis-a (**panels C** and **D**) in the presence of minimal or 100 nM free Ca^{+2}. Mibefradil is a Ca^{+2} channel blocker w/higher affinity for T-type (Kd = 0.1–4.7 μM) than L-type (Kd = 1.4–28 μM) Ca^{+2} channels. Hence, 0.5 and 1 μM of mibefradil discriminate T-type from L-type Ca^{+2} channels. Note that no inhibition of $[Ca^{+2}]_i$ levels are detected using either 0.5 or 1 μM mibefradil. There is no significant difference ($P < 0.1$) between the peaks of control and each dosage of mibefradil in any panel.

GTPases in the presence of L-selectin ligands happens within 5 min [Freeman et al., 2002]. Therefore, the transient $[Ca^{+2}]_i$ increase may mediate the Rho small GTPases activity in Sertoli cells and, in turn, act to regulate subsequent remodeling of the Sertoli cell cytoskeleton during the spermatogenic cycle.

Similar to activation of L-selectin by specific ligands, cross-linking of L-selectin with L-selectin antibodies has also been demonstrated to induce L-selectin-activated intracellular signals, including $[Ca^{+2}]_i$ increase, in leukocytes [Waddell et al., 1994; Crockett-Torabi and Fantone, 1997; Ding et al., 2003]. No data have been published, however, describing such an effect in Sertoli cells or cell lines derived from Sertoli cells. Therefore, anti-selectin experiments were performed to determine if cross-linking of Sertoli cell surface L-selectin receptors could also trigger an increase of intracellular Ca^{+2} level. Our data do demonstrate an increase of intracellular Ca^{+2} level in the presence of appropriate anti-L-selectins.

There are at least two possible mechanisms regarding the observed increase of intracellular Ca^{+2} levels. A change in intracellular ion concentration could result from either Ca^{+2} influx through the Sertoli cell membrane or release of internal stored Ca^{+2}. Clearly, both alterations may act concurrently. Ca^{+2} influx from the extracellular environment would necessarily be mediated by voltage-sensitive calcium channel proteins in the plasma membrane. Among the six classes of VOCCs, both L- and T-type VOCCs have been found in Sertoli cells involved in various signal transduction pathways [Gorczynska and Handelsman, 1991; Wassermann et al., 1992b; Foresta et al., 1995]. Although a few reports exist regarding the presence of N-, P-, and Q-type VOCCs, which are thought to be expressed only in the nervous system, on Sertoli cell membranes, these calcium channels have not been extensively studied [Ertel et al., 2000; Fragale et al., 2000; Barone et al., 2005]. Therefore, to clarify whether the cytosolic Ca^{+2} level increase

induced by L-selectin activation is indeed at least partially regulated by cell surface ion channels, L- and T-type VOCCs were examined by using Ca^{+2} channel blockers specific for either type. Our data demonstrate that intracellular Ca^{+2} level increases triggered by L-selectin ligation is abolished by the L-type VOCC blockers. T-type VOCCs do not seem to be implicated in the cellular response. In spite of the major effect of L-type VOCCs shown here, other types of Sertoli cell-surface Ca^{+2} channels, including other VOCCs and voltage-independent Ca^{+2} channels, might also have potential roles responsible for the Ca^{+2} influx induced by L-selectin activation [Grasso and Reichert, 1989, Gorczynska and Handelsman, 1991]. Involvement of these additional ion channels might explain why we detect incomplete inhibition of ion influx in the presence of the L-type VOCC blockers, nifedipine, diltiazem, and verapamil.

Experiments in this study were performed using cuvette-based spectrofluorimetry. Hence, data are measurements of overall fluorescence intensity changes observed from suspended cell populations. Spectrofluorimetry is indeed informative and time-saving, but limitations such as the inability to observe and quantify Ca^{+2} influxes of individual cell must be acknowledged. In addition, spectrofluorimetry cannot distinguish adequately between changes in intracellular Ca^{+2} levels caused by transmembrane flux or re-distribution of internal cellular ion pools. Certainly, some of the alterations we note in response to activation of L-selectin may be caused by release of intracellular Ca^{+2} from, for example, the endoplasmic reticulum. To address this important issue, we are currently conducting real-time morphological determinations of calcium changes using confocal immunofluorescent microscopy. Nevertheless, the inhibition noted using multiple blockers of VOCCs indicates that transmembrane influx does indeed result from activation of cell surface L-selectin.

Individual cells may vary greatly with regard to their response to activation of cell surface L-selectin. This is of particular potential importance when considering Sertoli cells of the testis. Sertoli undergo dramatic and cyclical alterations in their overall morphology, biosynthetic capability, and secretory functions as they progress through the spermatogenic cycle. Based upon substantial existing data, it is reasonable to assume that Sertoli cells isolated from different areas of seminiferous tubules, operating at distinct stages of the spermatogenic cycle, will have differential responses to L-selectin ligation or cross-linking. Therefore, real-time quantitative imaging of individual Sertoli cells is the next logical experimental approach in the analysis of the interactive role of L-selectin and calcium ions in the regulation of Sertoli cell function.

Rho small GTPases (Rho, Rac, and Cdc42) are important regulators of microfilament dynamics and cell–cell adhesion. Intriguingly, Ca^{+2} also regulates these pathways and processes involving these proteins often coincide with Rho GTPase-regulated pathways, and there are increasing observations that they might be linked [Ridley, 2001; Briggs and Sacks, 2003]. Several reports have specifically aimed to study the Ca^{+2}-upregulated Rho small GTPase signaling pathways [Ho et al., 1999; Liu et al., 2005]. Previous data from our lab suggests the activation of Rho family small GTPases (RhoA and Rac1) when exposed to known L-selectin ligands [Freeman et al., 2002]. However, the role of Ca^{+2} influx induced by L-selectin activation played between the L-selectin- Rho small GTPases pathway in Sertoli cells has never been investigated. Therefore, the relationship of the triggered Ca^{+2} influx to subsequent L-selectin-dependent upregulation of activated Rho small GTPases represents a logical extension of the results reported here.

In summary, our results demonstrate that activation of Sertoli cell surface L-selectin ligation by its ligand or by crosslinking of L-selectin with appropriate anti-L-selectin trigger a transient Ca^{+2} influx. Results also demonstrate that the L-type VOCC is at least partially responsible for the resultant Ca^{+2} influx. This is the first demonstration of L-selectin-induced intracellular Ca^{+2} shifts within Sertoli cells and also the first mechanistic evaluation of the Sertoli cell surface VOCC regulation during L-selectin activation.

ACKNOWLEDGMENTS

We thank Purnima Jani, MA for her expert assistance and companionship in the completion of this work. We also appreciate the advice and consultation provided by Dr. Kenneth Walsh, PhD.

REFERENCES

Balema O, Salter M, Heppner T, Bonev A, Nelson M, Mawe G. 2006. Spontaneous electrical rhythmicity and the role of the sarcoplasmic reticulum in the excitability of guinea pig gallbladder smooth muscle cells. Am J Physiol Gastrointest Liver Physiol 290:G655–G664.

Barone F, Aguanno S, D'Agostino A. 2005. Modulation of MAA-induced apoptosis in male germ cells: Role of Sertoli cell P/Q-type calcium channels. Reprod Biol Endocrinol 3:13.

Brenner B, Gulbins E, Busch G, Koppenhoefer U, Lang F, Linderkamp O. 1997. L-selectin regulates actin polymerisation via activation of the small G-protein Rac2. Biochem Biophys Res Commun 231:802–807.

Briggs M, Sacks D. 2003. IQGAP1 as signaling intergrator: Ca^{2+}, calmodulin, Cdc42, and the cytoskeleton. FEBS Lett 542:7–11.

Broome A, Abhayawardane Y, Morris R, Boockfor F, Millette C. 1997. L-Selectin is expressed by ASC17D Cells, MSC1 Cells, and adult and immature rat Sertoli cells. Mol Biol Cell 8S:323a.

Butcher E. 1991. Leukocyte-endothelial cell recognition: Three (or more) steps to specificity and diversity. Cell 67:1033–1036.

Crockett-Torabi E, Fantone J. 1997. L-selectin stimulation of canine neutrophil initiates calcium signal secondary to tyrosine kinase activation. Am J Physiol 272:H1302–H1308.

Ding Z, Issekutz T, Downey G, Waddell T. 2003. L-selectin stimulation enhances functional expression of surface CXCR4 in lymphocytes: Implications for cellular activation during adhesion and migration. Blood 101:4245–4252.

Ertel S, Ertel E, Clozel J. 1997. T-Type Ca^{2+} channels and pharmacological blockade: Potential pathophysiological relevance. Cardiovasc Drugs Ther 11:723–739.

Ertel E, Campbell K, Harpold M, Hofmann F, Mori Y, Perez-Reyes E, Schwartz A, Snutch T, Tanabe T, Birnbaumer L, Tsien R, Catterall W. 2000. Nomenclature of voltage-gated calcium channels. Neuron 25:533–535.

Fagnen G, Phamantu N, Bocquet J, Bonnamy P. 1999. Inhibition of transmembrane calcium influx induces decrease in proteoglycan synthesis in immature rat Sertoli Cells. J Cell Biochem 76:322–331.

Foresta C, Rossato M, Bordon P, Di Virgilio F. 1995. Extracellular ATP activates different signalling pathways in rat Sertoli cells. Biochem J 311:269–274.

Fragale A, Aguanno S, Kemp M, Reeves M, Price K, Beattie R, Craig P, Volsen S, Sher E, D'Agostino A. 2000. Identification and cellular localisation of voltage-operated calcium channels in immature rat testis. Mol Cell Endocrinol 162:25–33.

Freeman E, Jani P, Millette C. 2002. Expression and potential function of Rho family small G proteins in cells of the mammalian seminiferous epithelium. Cell Commun Adhes 9:189–204.

Gorczynska E, Handelsman D. 1991. The role of calcium in follicle-stimulating hormane signal transduction in Sertoli cells. J Biol Chem 266:23739–23744.

Grasso P, Reichert LJ. 1989. Follicle-stimulating hormone receptor-mediated uptake of $45Ca^{2+}$ by proteoliposomes and cultured rat sertoli cells: Evidence for involvement of voltage-activated and voltage-independent calcium channels. Endocrinology 125:3029–3036.

Ho Y, Joyal J, Li Z, Sacks D. 1999. IQGAP1 integrates Ca2+/calmodulin and Cdc42 signaling. J Biol Chem 274: 464–470.

Kansas G, Pavalko F. 1996. The cytoplasmic domains of E- and P-selectin do not constitutively interact with alpha-actinin and are not essential for leukocyte adhesion. J Immunol 157:321–325.

Lalevee N, Pluciennik F, Joffre M. 1997. Voltage-dependent calcium current with properties of T-type current in Sertoli cells from immature rat testis in primary cultures. Biol Reprod 56:680–687.

Laudanna C, Constantin G, Baron P, Scarpini E, Scarlato G, Cabrini G, Dechecchi C, Rossi F, Cassatella M, Berton G. 1994. Sulfatides trigger increase of cytosolic free calcium and enhanced expression of tumor necrosis factor-alpha and interleukin-8 mRNA in human neutrophils. Evidence for a role of L-selectin as a signaling molecule. J Biol Chem 269:4021–4026.

Ley K. 2003. The role of selectins in inflammation and disease. Trends Mol Med 9:263–268.

Liu C, Zuo J, Pertens E, Helli P, Janssen L. 2005. Regulation of Rho/ROCK signaling in airway smooth muscle by membrane potential and $[Ca^{2+}]_i$. Am J Physical Lung Cell Mol Physiol 289:L574–582.

Lyles G, Birrell C, Banchelli G, Pirisino R. 1998. Amplification of alpha 1D-adrenoceptor mediated contractions in rat aortic rings partially depolarised with KCl. Pharmacol Res 37:437–454.

Lyng F, Jones G, Rommerts F. 2000. Rapid androgen actions on calcium signaling in rat sertoli cells and two human prostatic cell lines: Similar biphasic responses between 1 picomolar and 100 nanomolar concentrations. Biol Reprod 63:736–747.

Martin R, Lee J, Cribbs L, Perez-Reyes E, Hanck D. 2000. Mibefradil block of cloned T-type calcium channels. J Pharmacol Exp Ther 295:302–308.

Mruk D, Cheng C. 2004. Sertoli-Sertoli and Sertoli-germ cell interactions and their significance in germ cell movement in the seminiferous epithelium during spermatogenesis. Endocr Rev 25:747–806.

Nebe B, Holzhausen C, Rychly J, Urbaszek W. 2002. Impaired mechanisms of leukocyte adhesion In vitro by the calcium channel antagonist mibefradil. Cardiovasc Drugs Ther 16:183–193.

Norgard-Sumnicht K, Varki N, Varki A. 1993. Calcium-dependent heparin-like ligands for L-selectin in nonlymphoid endothelial cells. Science 261:480–483.

O'Connell D, Koenig A, Jennings S, Hicke B, Han H, Fitzwater T, Chang Y, Varki N, Parma D, Varki A. 1996. Calclium-dependent oligonucleotide antagonists specific for L-selectin. Proc Nalt Acad Sci USA 93:5883–5887.

Okanlawon A, Dym M. 1996. Effect of chloroquine on the formation of tight junctions in cultured immature rat Sertoli cells. J Androl 17:249–255.

Parys J, Vanlingen S, Raeymaekers L, De Smedt H, Missiaen L. 2000. Subcellular fraction and intracellular calcium store. In: Putney JJ, editor. "Calcium signaling." Boca Raton, FL: CRC Press. pp 71–110.

Pavalko F, Walker D, Graham L, Goheen M, Doerschuk C, Kansas G. 1995. The cytoplasmic domain of L-selectin interacts with cytoskeletal proteins via alpha-actinin: receptor positioning in microvilli does not require interaction with alpha-actinin. J Cell Biol 129:1155–1164.

Ridley A. 2001. Rho family proteins: Coordinating cell responses. Trends Cell Biol 11:471–477.

Roberts K, Banerjee P, Tindall J, Zirkin B. 1995. Immortalization and characterization of a Sertoli cell line from the adult rat. Biol Reprod 53:1446–1453.

Roberts A, Kim C, Zhen L, Lowe J, Kapur R, Petryniak B, Spaetti A, Pollock J, Borneo J, Bradford G, Atkinson S, Dinauer M, Williams D. 1999. Deficiency of the hematopoietic cell-specific Rho family of GTPase Rac2 is characterized by abnormalities in neutrophil function and host defense. Immunity 10:183–196.

Simon S, Green C. 2005. Molecular mechanics and dynamics of leukocyte recruitment during inflammation. Annu Rev Biomed Eng 7:151–185.

Springer T. 1994. Traffic signals for lymphocyte recirculation and leukocyte emigration: the multistep paradigm. Cell 76:301–314.

Taranta A, Teti A, Stefanini M, D'Agostino A. 2000. Immediate cell signal induced by laminin in rat sertoli cells. Matrix Biol 19:11–18.

Tedder T, Steeber D, Chen A, Engel P. 1995. The selectins: Vascular adhesion molecules. FASEB J 9:866–873.

Thomas G, Sanderson J, Duncan G. 1999. Thapsigargin inhibits a potassium conductance and stimulates calcium influx in the intact rat lens. J Physiol 516:191–199.

Touyz R, Jiang L, Sairam M. 2000. Follicle-stimulating hormone mediated calcium signaling by the alternatively spliced growth factor type I receptor. Biol Reprod 62: 1067–1074.

Volpato K, Menegaz D, Leite L, Barreto K, de Vilhena Garcia E, Silva F. 2004. Involvement of K+ channels and calcium-dependent pathways in the action of T3 on amino acid accumulation and membrane potential in Sertoli cells of immature rat testis. Life Sci 74:1277–1288.

Waddell T, Fialkow L, Chan C, Kishimoto T, Downey G. 1994. Potentiation of the oxidative burst of human neutrophils. A signaling role for L-Selectin. J Biol Chem 269:18485–18491.

Waddell T, Fialkow L, Chan C, Kishimoto T, Downey G. 1995. Signaling functions of L-selecint. Enhancement of tyrosine phosphorylation and activation of MAP kinase. J Biol Chem 270:15403–15411.

Wassermann G, Monti Bloch L, Grillo M, Silva F, Loss E, McConnell L. 1992a. Electrophysiological changes of Sertoli cells produced by the acute administration of amino acid and FSH. Horm Metab Res 24:326–328.

Wassermann G, Bloch L, Grillo M, Silva G, Loss E, McConnell L. 1992b. Biochemical factors involved in the FSH action on amino acid transport in immature rat testes. Horm Metab Res 24:276–279.